Towards analytic description of a transition from weak to strong coupling regime in correlated electron systems. I. Systematic diagrammatic theory with two-particle Green functions

V. Janiš
Institute of Physics, Academy of Sciences of the Czech Republic,
Na Slovance 2, CZ-18040 Praha 8, Czech Republic
(February 1, 2008)

We analyze behavior of correlated electrons described by Hubbard-like models at intermediate and strong coupling. We show that with increasing interaction a pole in a generic two-particle Green function is approached. The pole signals metal-insulator transition at half filling and gives rise to a new vanishing "Kondo" scale causing breakdown of weak-coupling perturbation theory. To describe the critical behavior at the metal-insulator transition a novel, self-consistent diagrammatic technique with two-particle Green functions is developed. The theory is based on the linked-cluster expansion for the thermodynamic potential with electron-electron interaction as propagator. Parquet diagrams with a generating functional are derived. Numerical instabilities due to the metal-insulator transition are demonstrated on simplifications of the parquet algebra with ring and ladder series only. A stable numerical solution in the critical region is reached by factorization of singular terms via a low-frequency expansion in the vertex function. We stress the necessity for dynamical vertex renormalizations, missing in the simple approximations, in order to describe the critical, strong-coupling behavior correctly. We propose a simplification of the full parquet approximation by keeping only most divergent terms in the asymptotic strong-coupling region. A qualitatively new, feasible approximation suitable for the description of a transition from weak to strong coupling is obtained.

I. INTRODUCTION

Tight-binding models of correlated electrons are expected to provide description of thermodynamic and spectral properties of the underlying system in weak as well as in strong coupling regimes. We have at our disposal relatively reliable techniques to describe the two extreme limits of weak and strong couplings in the archetypal Anderson impurity and Hubbard lattice models. The weak-coupling regime is governed by a Hartree-Fock mean field with dynamical fluctuations captured by Fermi-liquid theory. Extended systems at low temperatures are Pauli paramagnets with smeared out local magnetic moments. For bipartite lattices antiferromagnetic long-range order sets on at half filling at arbitrarily small interaction. In the strong-coupling regime the Hubbard model at half filling maps onto a Heisenberg antiferromagnet with pronounced local magnetic moments and the Curie-Weiss law for the staggered magnetic susceptibility, at least at the mean-field level. The spectral structure is dominated by separated lower and upper Hubbard bands and the strongly correlated system seems to be insulating even in the paramagnetic phase.

In recent years importance of the regime, where the effective Coulomb repulsion is comparable with the kinetic energy and hence neither very weak nor very strong, has significantly increased. Unfortunately there is up to now no adequate method for the description of this transition regime between the weak and strong-coupling limits. At intermediate coupling dynamical fluctuations control the low-temperature physics of interacting electrons and neither weak-coupling nor atomic-like perturbation theories are adequate. In this nonperturbative regime we expect the Kondo regime to set on in the Anderson impurity model [1] and eventually breakdown of the Fermi-liquid regime and metal-insulator transition in the Hubbard model [2].

New progress in the construction of dynamical mean-field theories via high spatial lattice dimensions pushed forward our possibilities to investigate the transition region between weak and strong coupling [3]. Although the spatial fluctuations are reduced in high dimensions, there is no restriction on quantum dynamical fluctuations important at intermediate coupling. Particularly the quantum Monte-Carlo technique in $d=\infty$ revealed a number of new features of the (disordered) Hubbard model at finite temperatures [4–7]. However, the quantum Monte-Carlo is restricted only to relatively high temperatures.

That is why an analytic method based on second-order perturbation theory, called IPT, was used to study the transition from weak to strong coupling at zero temperature [8]. IPT at half filling reproduces well the finite-temperature Monte-Carlo data and contains the weak-coupling (up to U^2) and atomic solutions as exact limits. Contrary to Hubbard-III-like theories it reproduces Fermi liquid at weak coupling. A metal-insulator transition was found at $U_c \approx 6/\pi\nu$, where ν is the DOS at the Fermi level [9–11]. Although IPT is an analytic theory, its solution can be reached only via iterations that depend on the initial value of the self-energy. When we start with $\Sigma^{(0)}(z) = 0$ the iterations converge for weak interaction to a metallic solution. If we start with $\Sigma^{(0)}(z) = \Sigma_{at}(z) = U^2/4z$ we end up with an insulating solution for sufficiently strong interaction. The IPT scheme fails to converge close to the metal-insulator critical point. Another reasoning had to be used to demonstrate the existence and character of the metal-insulator transition [12].

At present IPT seems to be the only analytical-numerical scheme interpolating between Fermi liquid at weak coupling and paramagnetic insulator at strong coupling in a frustrated system, where the antiferromagnetic order is suppressed. However, the solution is numerically unstable in the most interesting region around the critical interaction. The quantitative details of the critical behavior at the metal-insulator transition and the way Fermi-liquid theory breaks down remain unaccessible. IPT is not a conserving theory and the two-particle functions, important for the description of inter-particle correlations, are not reliable in the IPT scheme. A systematic, consistent, and controllable theory delivering quantitative description of the critical behavior at the metal-insulator transition is still missing.

The aim of this paper is to fill up this gap and to develop a systematic theory interpolating between Fermi-liquid and local-moment regimes suitable for the description of the critical behavior at the metal-insulator transition of the Hubbard model or the Kondo behavior in the single-impurity Anderson model. We start with weak-coupling, self-consistent perturbation theory and propose a scheme how to extrapolate it to strong coupling. Contrary to IPT we concentrate on the two-particle Green functions showing divergence at the metal-insulator transition. We develop a systematic renormalized perturbation theory based on parquet-type diagrams with nontrivial renormalizations of two-particle functions. Especially we demonstrate the necessity for dynamical vertex renormalization whenever we approach a critical point. A theory with sufficient vertex renormalization is derived to describe the critical region of the metal-semimetal transition with condensation of bound electron-hole pairs. It is a simplified version of the parquet algebra keeping only most divergent contributions to the two-particle scattering function diverging at the critical point. It strongly renormalizes scatterings within singlet electron-hole pairs and leaves inter-pair and triplet correlations unrenormalized. To stabilize the numerical solution in the critical region the two-particle pole is factorized in the spirit of the renormalization group. The singular contributions can then be integrated analytically. The resultant new equations allow for a numerically stable solution even in the critical region of the condensation of bound electron-hole pairs. Such a method of numerical evaluation is asymptotically exact in the critical region of effective impurity models within the chosen approximation and makes tractable otherwise inaccessible diagram sums renormalizing the coupling constant far beyond simple ladder or ring series.

The layout of the paper is as follows. Section II analyzes the reasons why numerical solutions of sample models break down when the electron-electron interaction becomes strong. A systematic perturbation theory for intermediate and strong coupling using two-particle functions is expounded in Sec. III. Simple approximations of ring and ladder diagrams are rederived as examples in Sec. IV. These simple approximations are used in Sec. V to demonstrate the existence of poles in two-particle functions impeding direct numerical continuation of weak-coupling solutions to the strong-coupling limit. Section VI demonstrates the necessity for vertex renormalizations in self-consistent theories around critical points in order to comply with a Ward identity binding charge renormalizations (vertices) to mass renormalizations (self-energy). A feasible approximation within parquet algebra with self-consistent vertex renormalizations suitable for the description of the transition from weak to strong coupling is derived in Sec. VII. Last Section VIII brings conclusions.

II. CORRELATED ELECTRONS AT INTERMEDIATE COUPLING

To study correlated electron systems at intermediate coupling quantitatively we will basically work parallelly with two sample models: the single-impurity Anderson and the lattice Hubbard models. The former one will serve as a test case for comparison of developed approximations with the exact Bethe-ansatz or numerical renormalization-group solution. The latter model will explicitly be studied only at

the mean-field level, i.e. in infinite spatial dimensions where spatial fluctuations are suppressed [13]. This enables us to cover both the model situations within one theoretical framework.

We start with the underlying Hamiltonians

$$\widehat{H}_{SIAM} = \sum_{\mathbf{k},\sigma} \epsilon(\mathbf{k}) c^\dagger_{\mathbf{k}\sigma} c_{\mathbf{k}\sigma} + \varepsilon_f \sum_\sigma f^\dagger_\sigma f_\sigma + U f^\dagger_\uparrow f_\uparrow f^\dagger_\downarrow f_\downarrow + \sum_{\mathbf{k},\sigma} \left[V_\mathbf{k} c^\dagger_{\mathbf{k}\sigma} f_\sigma + V^*_\mathbf{k} f^\dagger_\sigma c_{\mathbf{k}\sigma} \right] \tag{1a}$$

for the single-impurity Anderson model and with

$$\widehat{H}_{HM} = \sum_{\mathbf{k},\sigma} \epsilon(\mathbf{k}) c^\dagger_{\mathbf{k}\sigma} c_{\mathbf{k}\sigma} + U \sum_\mathbf{i} c^\dagger_{\mathbf{i}\uparrow} c_{\mathbf{i}\uparrow} c^\dagger_{\mathbf{i}\downarrow} c_{\mathbf{i}\downarrow} \tag{1b}$$

for the Hubbard model. In the former case we integrate out the conduction electrons and transform the model onto a single-site theory with dynamical localized electrons. The interaction dependent partition sum has form of a local functional integral

$$\mathsf{Z}_{Loc} = \int \mathcal{D}f\mathcal{D}f^* \exp\left\{ \sum_{\sigma,n} f^*_{\sigma n} \mathcal{G}^{-1}_{\sigma n} f_{\sigma n} - U \int_0^\beta d\tau f^*_\uparrow(\tau) f_\uparrow(\tau) f^*_\downarrow(\tau) f_\downarrow(\tau) \right\} \tag{2a}$$

where

$$\mathcal{G}^{-1}_{\sigma n} = i\omega_n + \mu_\sigma - \varepsilon_f - V^2 G_\sigma(i\omega_n) \ , \quad G^{(0)}_\sigma(z) = \int d\epsilon \rho(\epsilon) [z + \mu_\sigma - \epsilon]^{-1} \tag{2b}$$

is the effective dynamical propagator of the localized electrons and $\mu_\sigma = \mu + \sigma h$. The variables f, f^* are Grassmann ones and ρ is the density of states of the conduction electrons.

The Hubbard model in infinite dimensions, i.e. at the mean-field level can be mapped onto an impurity problem self-consistently embedded in an averaged medium [14,8]. The partition sum can then be transformed onto a local functional integral identical with (1a) where only the effective dynamical propagator is defined as

$$\mathcal{G}^{-1}_{\sigma n} = G^{-1}_{\sigma n} + \Sigma_{\sigma n} \ , \quad G_{\sigma n} = \int d\epsilon \rho(\epsilon) [i\omega_n + \mu_\sigma - \Sigma_{\sigma n} - \epsilon]^{-1} \tag{2c}$$

with $\Sigma_{\sigma n}$ as the self-energy to be determined from an equation

$$G_{\sigma n} = \frac{1}{\mathsf{Z}_{Loc}} \int \mathcal{D}f\mathcal{D}f^* f^*_{\sigma n} f_{\sigma n} \exp\left\{ \sum_{\sigma,n} f^*_{\sigma n} \mathcal{G}^{-1}_{\sigma n} f_{\sigma n} - U \int_0^\beta d\tau f^*_\uparrow(\tau) f_\uparrow(\tau) f^*_\downarrow(\tau) f_\downarrow(\tau) \right\} . \tag{2d}$$

The physics of both the sample systems is determined completely from the effective local but dynamical partition sum Z_{Loc}. Here the unperturbed propagator is $\mathcal{G}$ and the only dynamical variable is the imaginary time $\tau \in (0, \beta)$ or Matsubara frequency $i\omega_n$.

Although the mathematical representation for the impurity Anderson and the mean-field Hubbard partition sum is formally identical, physical behavior of these models at intermediate coupling is expected to be different. The impurity model remains local Fermi liquid up to infinite interaction strength [15]. At half filling a quasiparticle peak forms around the Fermi energy ($E_F = 0$) in the density of states of the local dynamical electrons the width of which is determined by a Kondo (dimensionless) scale

$$\Delta = \exp\{-\pi U \nu\} \tag{3}$$

and a typical energy of the model (e.g. the bandwidth of the conduction electrons). It is the existence of this Kondo scale incomparably smaller than other scales of the underlying Hamiltonian that makes perturbation expansion fail at intermediate coupling. Except for asymptotically exact solutions in the low-energy limit such as Bethe-ansatz [16] or numerical renormalization group [17], there is no other reliable approximate scheme being able to reproduce the Kondo strong-coupling asymptotics (3) [18].

Recent studies on the Hubbard model in $d = \infty$ show that the Kondo scale of the impurity model should vanish at a critical interaction ($U_c \approx 6\pi/\nu$) due to the additive self-consistency between the "unperturbed" propagator $\mathcal{G}$ and the self-energy [9–12]. The electronic system undergoes a metal-insulator

transition. Fermi-liquid theory and weak-coupling perturbation expansions break down at this transition. Breakdown of perturbation theory at the Mott metal-insulator transition is not caused by the exponentially small Kondo scale but by the divergence of the effective mass determining criticality of the metal-insulator transition at zero temperature. Effective mass is connected with the real part of the self-energy $m^*/m \propto 1 - \Sigma'$ where $\Sigma' = \partial\Sigma(\omega)/\partial\omega|_{\omega=0}$. Divergence of the effective mass also causes vanishing of an energy scale. This energy scale is determined by frequencies $\omega_\pm$ at which the real part of the self-energy reaches its extremum closest to the Fermi energy. These frequencies determine an energy interval around the Fermi level within which Fermi liquid and the quasiparticle picture is applicable. Fig. 1 shows $\mathrm{Re}\Sigma(\omega)$ calculated within self-consistent ring diagrams. It is clearly seen that $\omega_\pm \to 0$ with increasing interaction strength. Vanishing of the difference between $\omega_+ > 0$ and $\omega_- < 0$ and arising of a jump in $\mathrm{Re}\Sigma(\omega)$ then lead to numerical instabilities and breakdown of iteration schemes to self-consistent approximations at intermediate coupling, disregarding whether they can or cannot describe the metal-insulator transition [19].

At intermediate coupling the two investigated models have a vanishing small scale in common. It causes numerical instabilities in self-consistent approximations and breakdown of iteration schemes [20]. It hinders analytic continuation of weak-coupling approximations to the strong-coupling limit. To succeed in quantitative description of intermediate coupling it is necessary to treat the vanishing "Kondo" scale separately from the other scales determined by the underlying Hamiltonians. To do that we must understand the origin of this scale. We will demonstrate in this paper that the vanishing scale reflects criticality of a two-particle (actually electron-hole) correlation function. It means that a two-particle Green function at intermediate coupling develops a pole at the Fermi energy. It is known from the early papers on the Kondo problem that the Kondo scale or the Kondo temperature is connected with an RPA pole in the magnetic susceptibility [21]. It was pointed out recently [9] that also at the metal-insulator transition the local, dynamical susceptibility shows divergence at the Fermi energy. In order to get the vanishing scale at intermediate coupling under control a systematic renormalized perturbation theory based on approximations for two-particle Green functions is to be used.

III. SYSTEMATIC SELF-CONSISTENT APPROXIMATIONS FOR TWO-PARTICLE GREEN FUNCTIONS

To develop systematic approximations for one-particle Green functions we use Dyson's equation enabling us to consider explicitly only one-particle irreducible diagrams contributing to the self-energy. The situation is more complicated at the level of two-particle functions. Although we can use a Bethe-Salpeter equation to extract two-particle irreducible diagrams, we have three possibilities to do it. We have three channels for multiple two-particle scatterings defining three types of two-particle irreducibility. They are the electron-hole (e-h), electron-electron (e-e), and interaction (U) channels schematically drawn in Fig. 2. Different channels mean different rearrangements of perturbation expansion. The chosen irreducible diagrams are summed first and the remaining reducible ones are summed via a Bethe-Salpeter equation in the end. If perturbation series converges all rearrangements must lead to the same result.

When studying two-particle functions we need to know the one-particle self-energy. Hence perturbation theory for two-particle functions cannot be developed without a parallel expansion for the self-energy. To approximate the one and two-particle functions simultaneously we use perturbation expansion with two-particle functions as a means for developing controllable comprehensive approximations for a generating thermodynamic potential. All the physical quantitities will then be determined consistently from the generating functional via functional derivatives.

As a first step we decide which is the relevant two-particle function for our purpose to describe intermediate and strong coupling. It should be a function approaching a pole with increasing interaction. Such a function must be related to the interaction (two-particle) part of the underlying Hamiltonian. The natural generalization of the Hubbard interaction is the following two-particle function

$$\mathcal{C}_{\mathbf{ij}}(\tau) = \langle \widehat{n}_{\mathbf{i}\uparrow}(\tau)\widehat{n}_{\mathbf{j}\downarrow}(0)\rangle - \langle \widehat{n}_{\mathbf{i}\uparrow}(\tau)\rangle\langle \widehat{n}_{\mathbf{j}\downarrow}(0)\rangle \tag{4}$$

measuring correlations between spin up and spin down densities at different times and different lattice sites. The brackets denote thermal average. Fourier transform $\mathcal{C}(\mathbf{q}, i\nu_m)$ of the above function is a two-particle function approaching a pole when the Hubbard interaction increases. Note that ν_m are

bosonic Matsubara frequencies. Due to the space and time translational invariance of the Hamiltonian, $\mathrm{Im}\mathcal{C}(\mathbf{q},0) = 0$ and the real part has definite sign, namely

$$\mathcal{C}(\mathbf{q},0) \propto -UX_\uparrow(\mathbf{q})X_\downarrow(\mathbf{q}) < 0 \quad \text{with} \quad X_\sigma(\mathbf{q}) = \mathcal{N}^{-1}\sum_{\mathbf{k}} \frac{f(\epsilon(\mathbf{k})-\mu_\sigma)-f(\epsilon(\mathbf{k}+\mathbf{q})-\mu_\sigma)}{\epsilon(\mathbf{k})-\epsilon(\mathbf{k}+\mathbf{q})} \,. \tag{5}$$

This relation is exactly fulfilled at weak-coupling and can qualitatively be broken (change of the sign) only if the function $\mathcal{C}(\mathbf{q},i\nu_m)$ goes thru a pole. The pole would indicate breakdown of Fermi liquid. In the weak-coupling, Fermi-liquid regime we can write

$$\mathcal{C}(\mathbf{q},0) = \frac{T}{4}\left[\kappa(\mathbf{q},0) - \chi(\mathbf{q},0)\right] < 0 \tag{6}$$

where $\kappa(\mathbf{q},i\nu_m)$ is the dynamical compressibility and $\chi(\mathbf{q},i\nu_m)$ the dynamical magnetic susceptibility. Eq. (6) states that magnetic fluctuations are stronger than charge fluctuations in the models with the Hubbard interaction. Divergence in the function $\mathcal{C}(\mathbf{q},0)$ induces divergence in the magnetic susceptibility and hence is indication of a magnetic long-range order.

Function $\mathcal{C}(\mathbf{q},i\nu_m)$ will be approximated by a selection of classes of Feynman diagrams. Consistency and conservation laws demand that a two-particle approximation be in concord with an approximation on the one-particle self-energy. According to Baym and Kadanoff [22,23] a conserving theory must work with fully renormalized one-particle propagators. Hence only fully self-consistent approximations are acceptable at the level of two-particle functions. To construct consistent approximation schemes we have to build up the generating functional $\Phi[U,G]$ using the function $\mathcal{C}(\mathbf{q},i\nu_m)$. To do that we apply a linked-cluster expansion recently proposed by the author and J. Schlipf [20]. Its salient feature is that the the interaction line (non-relativistic photons) is used for edges (diagram bonds or propagators) and loops of electron Green functions serve as unperturbed vertices. An analogy between the classical free-energy functional of the Ising model $W[J,h]$ and the quantum grand potential $\Omega[U,G^{(0)}]$ is thereby made, i.e. $J \longleftrightarrow U$ and $h \longleftrightarrow G^{(0)}$. We use this analogy to construct the generating functional $\Phi[U,G]$ from the two-particle Green function $\mathcal{C}(\mathbf{q},i\nu_m)$.

We represent the grand potential of the Hubbard model in the homogeneous phase in the following form

$$\begin{aligned}\frac{1}{\mathcal{N}}\Omega[n;\Sigma,G] = -Un_\uparrow n_\downarrow - \frac{1}{\beta\mathcal{N}}\sum_{\sigma n,\mathbf{k}} e^{i\omega_n 0^+}\, &\{\ln\left[i\omega_n + \mu_\sigma - \epsilon(\mathbf{k}) - Un_{-\sigma} - \Sigma_\sigma(\mathbf{k},i\omega_n)\right] \\ &+G_\sigma(\mathbf{k},i\omega_n)\Sigma_\sigma(\mathbf{k},i\omega_n)\} + \Phi[U,G]\,,\end{aligned} \tag{7}$$

where $n_\sigma, \Sigma_\sigma(\mathbf{k},i\omega_n), G_\sigma(\mathbf{k},i\omega_n)$ are variational variables (functions). We now introduce a small perturbation $U \to U + \delta U(\mathbf{q},i\nu_m)$. The function $\mathcal{C}(\mathbf{q},i\nu_m)$ is defined as a variational derivative of the generating functional

$$\mathcal{C}(U;\mathbf{q},i\nu_m) = \left.\frac{\delta\Phi\left[U,G\right]}{\delta U(\mathbf{q},i\nu_m)}\right|_{\delta U=0} . \tag{8}$$

Linked-cluster theorem can be used for the inverse transformation

$$\Phi[U,G] = \frac{U}{\beta\mathcal{N}}\sum_{\mathbf{q}m}\int_0^1 d\lambda\,\mathcal{C}(U\lambda|\mathbf{q},i\nu_m)\,. \tag{9}$$

Two-particle function $\mathcal{C}(U\lambda|\mathbf{q},i\nu_m)$ is understood as a functional of the full renormalized electron propagator $G(\mathbf{k},i\omega_n)$ with the self-energy determined at the interaction strength U.

Function $\mathcal{C}(U|\mathbf{q},i\nu_m)$ does not directly obey an equation of motion. It is connected with a general two-particle Green function $\mathcal{K}_{\uparrow\downarrow}(U|k',k'';q)$ determined from a set of coupled Bethe-Salpeter equations. To simplify lengthy expressions we sometimes use a four-vector notation $k = (\mathbf{k},i\omega_n)$ and $q = (\mathbf{q},i\nu_m)$ for fermionic and bosonic variables, respectively. We can write

$$\mathcal{C}(U|\mathbf{q},i\nu_m) = \frac{1}{\beta^2\mathcal{N}^2}\sum_{k',k''} G_\uparrow(k')G_\uparrow(k'+q)G_\downarrow(k'')G_\downarrow(k''+q)\mathcal{K}_{\uparrow\downarrow}(U|k',k'';q)\,. \tag{10}$$

Functions $\mathcal{K}_{\sigma\sigma'}(k',k'';q)$ can be represented as a sum of contributions from different two-particle channels

$$\mathcal{K}_{\sigma\sigma'}(k,k';q) = I_{\sigma\sigma'}(k,k';q) + \mathcal{K}^{U}_{\sigma\sigma'}(k,k';q) + \mathcal{K}^{eh}_{\sigma\sigma'}(k,k';q) + \mathcal{K}^{ee}_{\sigma\sigma'}(k,k';q) \tag{11}$$

where $I_{\sigma\sigma'}$ contains diagrams *irreducible* in all the channels while $\mathcal{K}^{\alpha}_{\sigma\sigma'}$ is a sum of diagrams *reducible* in the particular channel α. Each of the reducible two-particle functions obeys a Bethe-Salpeter equation mixing all the channels and eventually spins. The equations in the "horizontal" electron-hole and electron-electron channels read

$$\begin{aligned}\mathcal{K}^{eh}_{\sigma\sigma'}(k,k';q) = -\frac{1}{\beta\mathcal{N}}\sum_{q'}\Lambda^{eh}_{\sigma\sigma'}(k,k';q')G_{\sigma}(k+q')G_{\sigma'}(k'+q')&\\ \mathcal{K}_{\sigma\sigma'}(k+q',k'+q';q-q')\,,&\end{aligned} \tag{12a}$$

$$\begin{aligned}\mathcal{K}^{ee}_{\sigma\sigma'}(k,k';q) = -\frac{1}{\beta\mathcal{N}}\sum_{k''}\Lambda^{ee}_{\sigma\sigma'}(k,k+k'+q-k'';k''-k)G_{\sigma}(k'')G_{\sigma'}(k+k'+q-k'')&\\ \mathcal{K}_{\sigma\sigma'}(k'',k';k+q-k'')\,.&\end{aligned} \tag{12b}$$

The reducible functions in the "vertical" or the interaction channel are determined from equations

$$\mathcal{K}^{U}_{\sigma\sigma'}(k,k';q) = -\frac{1}{\beta\mathcal{N}}\sum_{k''\sigma''}\Lambda^{U}_{\sigma\sigma''}(k,k'';q)G_{\sigma''}(k'')G_{\sigma''}(k''+q)\mathcal{K}_{\sigma''\sigma'}(k'',k';q)\,. \tag{12c}$$

Here $\Lambda^{\alpha}_{\sigma\sigma'}(k,k';q)$ are sums of irreducible diagrams in the α-th channel. Equations (12) have the structure of parquet diagrams [24,25]. To complete the parquet algebra and to close the equations we must add a definition for the irreducible functions from each channel. When no further approximations are used the parquet equations are completed with a relation between reducible, $\mathcal{K}^{\alpha}$, and irreducible, Λ^{α} functions

$$\Lambda^{\alpha}_{\sigma\sigma'}(k',k'';q') = \mathcal{K}_{\sigma\sigma'}(k',k'';q) - \mathcal{K}^{\alpha}_{\sigma\sigma'}(k',k'';q)\,. \tag{13}$$

The generating functional $\Phi[U,G]$ is now fully determined from the completely irreducible two-particle vertex functions $I_{\sigma\sigma'}(U\lambda|k',k'';q)$, Bethe-Salpeter equations (11)- (13), and the linked-cluster theorem (9), with (10). The self-energy is determined from the saddle-point of the generating functional Ω with respect to the fermion propagator G. Note that the self-energy here measures only dynamical fluctuations beyond the Hartree approximation. Even the simplest approximations on the scattering matrix $\mathcal{K}_{\uparrow\downarrow}$ lead to nontrivial complex structure of two-particle functions causing the existence of poles at strong coupling.

IV. SIMPLE APPROXIMATIONS

As examples of the general construction we derive a few simple approximations where we can get rid of the integral over the interaction strength and calculate all the quantities at the same value of the coupling constant U. In all these approximations the completely irreducible vertex $I_{\uparrow\downarrow}$ is assumed to be the bare interaction U.

A. Ring diagrams

We neglect contributions to the two-particle scattering matrix $\mathcal{K}_{\uparrow\downarrow}$ coming from the electron-electron and electron-hole channels and consider explicitly only the interaction channel. It means that no multiple scatterings are allowed. Further on we neglect the irreducible functions for scatterings of quasiparticles with the same spin. The two-particle function $\mathcal{K}_{\uparrow\downarrow}$ in this approximation then reads

$$\mathcal{K}^{Ring}_{\uparrow\downarrow}(U|k',k'';q) = \frac{U}{1-U^2X_{\uparrow}(\mathbf{q},i\nu_m)X_{\downarrow}(\mathbf{q},i\nu_m)}\,. \tag{14}$$

The integral over the interaction strength can simply be performed leading to a generating functional

$$\Phi^{Ring}[U,G](\mathbf{q},i\nu_m) = \frac{1}{2\beta\mathcal{N}}\sum_{\mathbf{q}m}e^{i\nu_m0^+}\ln\left[1-U^2X_{\uparrow}(\mathbf{q},i\nu_m)X_{\downarrow}(\mathbf{q},i\nu_m)\right] \tag{15a}$$

where

$$X_\sigma(\mathbf{q}, i\nu_m) = \frac{1}{\beta\mathcal{N}} \sum_{\mathbf{k}n} G_\sigma(\mathbf{k}, i\omega_n) G_\sigma(\mathbf{k}+\mathbf{q}, i(\omega_n + \nu_m)) \tag{15b}$$

is a bubble of two full one-electron propagators. The self-energy can easily be derived in form of an integral equation

$$\begin{aligned}\Sigma^{Ring}(\mathbf{k}, i\omega_n) = -\frac{U^2}{2\beta\mathcal{N}} \sum_{\mathbf{q}m} &[G_\sigma(\mathbf{k}+\mathbf{q}, i(\omega_n + \nu_m)) \\ &+G_\sigma(\mathbf{k}-\mathbf{q}, i(\omega_n - \nu_m))] \frac{X_{-\sigma}(\mathbf{q}, i\nu_m)}{1 - U^2 X_\uparrow(\mathbf{q}, i\nu_m) X_\downarrow(\mathbf{q}, i\nu_m)} \,.\end{aligned} \tag{15c}$$

We have a complete set of integral equations the solution of which fully determines thermodynamic as well as spectral properties of the self-consistent ring-diagram approximation. If we reduce this approximation to infinite dimensions, the full extended propagator is replaced by its local element, we reveal a mean-field version of the ring diagrams recently studied numerically [26,20]. At the mean-field level the numerics breaks down at intermediate filling ($U \approx 6/\pi\nu$) when the pole in $C(z)$ is approached [19]. We expect the same for the finite-dimensional version, but the pole will appear at a specific wave vector $\mathbf{q}_0$.

B. Ladder diagrams

Next step in developing approximations onto two-particle scattering matrix $\mathcal{K}_{\uparrow\downarrow}$ is to consider ladders of either multiple electron-hole or electron-electron scatterings by neglecting the contributions from the interaction channel. In these ladder approximations we neglect screening of the interaction due to polarization bubbles of electron-hole pairs. Summing the geometric series of the Bethe-Salpeter equations we obtain for the electron-hole channel

$$\mathcal{K}^{RPA}_{\uparrow\downarrow}(U|k,k';q) = \frac{U}{1 + \frac{U}{\beta\mathcal{N}} \sum_{k''} G_\uparrow(k - k' + k'') G_\downarrow(k'')} \tag{16a}$$

and for the electron-electron channel

$$\mathcal{K}^{TMA}_{\uparrow\downarrow}(U|k,k';q) = \frac{U}{1 + \frac{U}{\beta\mathcal{N}} \sum_{k''} G_\uparrow(k + k' - k'') G_\downarrow(k'')} \,. \tag{16b}$$

We can again perform the integration in the linked-cluster theorem (9) and end up with

$$\Phi^{RPA}[U, G] = -\frac{1}{\beta\mathcal{N}} \sum_{\mathbf{q}m} e^{i\nu_m 0^+} \left\{ UX(\mathbf{q}, i\nu_m) - \ln[1 + UX(\mathbf{q}, i\nu_m)] \right\} \tag{17a}$$

for the electron-hole channel and analogously with

$$\Phi^{TMA}[U, G] = -\frac{1}{\beta\mathcal{N}} \sum_{\mathbf{q}m} e^{i\nu_m 0^+} \left\{ UY(\mathbf{q}, i\nu_m) - \ln[1 + UY(\mathbf{q}, i\nu_m)] \right\} \tag{17b}$$

for the electron-electron channel. Here we denoted

$$X(\mathbf{q}, i\nu_m) = \frac{1}{\beta\mathcal{N}} \sum_{\mathbf{k}n} G_\uparrow(\mathbf{q}+\mathbf{k}, i\omega_{m+n}) G_\downarrow(\mathbf{k}, i\omega_n) \,, \tag{17c}$$

$$Y(\mathbf{q}, i\nu_m) = \frac{1}{\beta\mathcal{N}} \sum_{\mathbf{k}n} G_\uparrow(\mathbf{q}-\mathbf{k}, i\omega_{m-n}) G_\downarrow(\mathbf{k}, i\omega_n) \,. \tag{17d}$$

Note that Φ^{RPA} generates random-phase approximation with renormalized propagators, i.e. its renormalized version as introduced by Suhl in the study of the single-impurity Anderson model [27]. The generating functional Φ^{TMA} with multiple electron-electron scatterings describes a renormalized T-matrix

approximation studied by Baym and Kadanoff [22]. The self-energies, respective their corrections to the Hartree approximation, for ladder diagrams read

$$\Sigma_\sigma^{RPA}(\mathbf{k}, i\omega_n) = -\frac{U^2}{\beta\mathcal{N}}\sum_{\mathbf{q}m} G_{-\sigma}(\mathbf{k}-\mathbf{q}, i\omega_{n-m})\frac{X(\mathbf{q}, i\nu_m)}{1+UX(\mathbf{q}, i\nu_m)}\,, \tag{17e}$$

$$\Sigma_\sigma^{TMA}(\mathbf{k}, i\omega_n) = -\frac{U^2}{\beta\mathcal{N}}\sum_{\mathbf{q}m} G_{-\sigma}(\mathbf{k}+\mathbf{q}, i\omega_{n-m})\frac{Y(\mathbf{q}, i\nu_m)}{1+UY(\mathbf{q}, i\nu_m)}\,. \tag{17f}$$

The ring and ladder diagrams constitute simplest approximations at the level of two-particle functions enabling for explicit analytic form of the generating functional Φ. These approximations are fully self-consistent and contain geometric series of two-particle bubbles. The ring diagrams use bubbles of electron-hole pairs of the same spin, while the RPA and TMA involve bubbles of quasiparticles with opposite spins. Due to the full self-consistency in these simple approximations it is in principle possible to find a solution in the whole range of the interaction strength. It is, however, necessary to stress that these approximations can be expected reliable only at weak coupling, since only diagrams to second order are treated exactly here. We use these approximations as samples to demonstrate breakdown of numerical iteration schemes at intermediate coupling and the necessity for a separate treatment of the new small scale connected with zero of the denominator of the two-particle functions from the self-energy equations.

V. TWO-PARTICLE CRITICALITY

To simplify the analysis we leave the general formulation and resort to a mean-field description. We suppress the momentum convolutions and come from the full momentum-dependent Green functions to their local parts. Further on we choose the spin-symmetric solution at zero temperature for the half-filled band. These assumptions lead to significant simplifications of the resultant equations and enable to trace down breakdown of perturbation theory at strong coupling of the lattice models.

We first analytically continue the equation for the self-energy to real frequencies and take explicit advantage of the electron-hole symmetry. Then the generic equation for the self-energy can be written as [19]

$$\Sigma(z) = \frac{U^2}{2}\int_{-\infty}^0 \frac{d\omega'}{\pi}\left\{\mathrm{Im}G(\omega'_+)\left[C(\omega'-z)-C(\omega'+z)\right] + \mathrm{Im}C(\omega'_+)\left[G(\omega'+z)-G(\omega'-z)\right]\right\} \tag{18a}$$

where

$$C^{Ring}(\zeta) = \frac{X(\zeta)}{1-U^2X(\zeta)^2}\,,\quad C^{RPA}(\zeta) = \frac{X(\zeta)}{1+UX(\zeta)}\,,\quad C^{TMA}(\zeta) = \frac{X(\zeta)}{1-UX(\zeta)}\,. \tag{18b}$$

The two-particle bubble X has a representation

$$X(\zeta) = -\int_{-\infty}^0 \frac{d\omega'}{\pi}\mathrm{Im}G(\omega'_+)\left[G(\omega'+\zeta)+G(\omega'-\zeta)\right]\,. \tag{18c}$$

Here z and ζ stand for complex energies in fermionic and bosonic functions, respectively.

Troubles with the numerical solution of these equations begin when the two-particle function $C(\zeta)$ approaches a pole at $\zeta = 0$. In analogy to the stability condition (5) this function must fulfill

$$C(0) < 0 \tag{19}$$

in order to keep the effective mass of the interacting electrons positive. When inequality (19) is broken, even by intermediate iterations, the numerical solution fails to converge or a solution on an unphysical sheet is reached. It is easy to verify that $X(0) < 0$ and hence only the RPA and ring diagrams run into troubles at intermediate coupling. The TMA is harmless and can be extrapolated to strong coupling without meeting numerical problems [28]. One can expect this, since due to the Coulomb repulsion the electron-hole pairs tend to bind. Multiple scatterings of electrons on electrons do not contribute to this

process. Only the ring and RPA diagrams are relevant for creation of electron-hole bound states and divergence of the effective electron mass at the metal-insulator transition.

The dynamical two-particle function C, the local element of the full correlation function $\mathcal{C}$, defines at intermediate coupling a new dimensionless scale

$$\Delta = 1 + UX(0) \to 0 \tag{20}$$

when its pole is approached. To determine the actual strong-coupling asymptotics of the RPA and ring diagrams it is necessary to calculate the behavior of the small scale Δ as a function of the interaction strength as accurate as possible. On the one hand the existence of this small scale impedes continuation of weak-coupling solutions to strong coupling. On the other hand vanishing of this scale at the critical point of the metal-insulator transition enables us to pick up divergent contributions in the critical region analytically. Only the low-frequency behavior of the two-particle function $C(\omega)$ is relevant in leading order of diverging effective mass. We can replace the full frequency dependence of the denominator of the function $C(\omega)$ by its low-frequency asymptotics. Such an approach to derivation of the strong-coupling asymptotics was used by Hamann [30] in the case of Suhl's renormalized RPA and recently by the author [19] for the ring diagrams. This treatment of the the singular function $C(\omega)$ is asymptotically exact at the critical point with nonintegrable singularity.

The existing asymptotic expansions for real frequencies can be generalized to the complex plane in such a way that the analytic structure of the resultant self-energy is not violated. No spurious poles are generated in the lower and upper half-planes of complex energies. This property is essential not to break the sum rules. We hence make the following low-frequency ansatz for the denominator of $C(\zeta)$ vanishing at the critical point

$$1 + UX(\zeta) \doteq \Delta - i\mathrm{sign}(\mathrm{Im}\zeta)UX'\zeta\,. \tag{21}$$

We introduced a new parameter X' as the only part of the function $X(\zeta)$ relevant for the critical behavior of the solution. It is easy to see that for the simple approximations

$$X' = \pi\nu^2 > 0 \tag{22}$$

where $\nu = \rho(0)$ remains unrenormalized in the Fermi-liquid regime. Hence the two-particle vertex does not dynamically renormalize in the low-frequency limit for simple ladder and ring diagrams.

We use ansatz (21) and simplify the equation for the self-energy by keeping only leading-order terms due to the singularity of $C(\zeta)$, i.e. in $|\ln\Delta|$. As a result we obtain two regions for the self-energy. For finite frequencies, $|z| \gg \Delta/UX'$ the solution reads

$$\Sigma^{Ring}(z) = \frac{1}{2}\Sigma^{RPA}(z) = -\frac{G(z)}{2\pi X'}\ln\Delta\,. \tag{23a}$$

In the limit of small frequencies, $|z| \approx \Delta/UX'$ the self-energy has another representation

$$\Sigma^{Ring}(z) = \frac{1}{2}\Sigma^{RPA}(z) = -\frac{G(z)}{2\pi X'}\ln\Delta + i\widehat{\eta}\frac{\mathrm{Im}G(i0^+)}{2\pi X'}\ln[\Delta - i\widehat{\eta}UX'z]\,. \tag{23b}$$

Formulas (23) hold for any external (complex) frequency $z = \omega + i\eta$ with $\widehat{\eta} = \mathrm{sign}\eta$. The solution has correct Fermi-liquid asymptotics for small as well as for large frequencies. Moreover, the Herglotz analytic properties of the self-energy are preserved.

To complete the equation for the self-energy we need to determine the parameter Δ. We use a representation $X(0) = 2\int_{-\infty}^{0} d\omega'\rho(\omega')\mathrm{Re}G(\omega')$ that can easily be evaluated from the derived asymptotic form of the self-energy. Only frequencies $0 > \omega > -\sqrt{|\ln\Delta|/\alpha\pi X'}$ are relevant, where $\alpha = 1, 2$ for RPA and ring diagrams, respectively. Using (23a) we finally obtain

$$X^{Ring}(0) = \sqrt{2}X^{RPA}(0) = \sqrt{\frac{2\pi X'}{|\ln\Delta|}}\,. \tag{24}$$

Note that the low-frequency asymptotics of the self-energy, (23b), is irrelevant for evaluation of the integral $X(0)$. It, however, determines the Fermi-liquid, quasiparticle characteristics of the solution. E.g. the effective mass comes out from (23b) as

$$\frac{m^*}{m} \propto \frac{U\nu}{\alpha\Delta}\,. \tag{25}$$

We know from earlier studies that Fermi liquid gets less and less thermodynamically important with increasing interaction, since the width of the energy interval around the Fermi level, within which Fermi-liquid (quasiparticle) picture holds shrinks to zero as $\Delta|\ln\Delta|$. Non-Fermi-liquid contributions, i.e. the frequencies beyond the first extremum in the real part of the self energy overtake the control over macroscopic, integral quantities [19,31].

From the definition of the parameter Δ, (20), and from (24) we obtain an asymptotic form for this two-particle scale

$$\Delta = \exp\{-\alpha\pi^2\nu^2U^2\} \tag{26}$$

the result derived for the first time by Hamann for the single-impurity Anderson model [30]. Our derivation of the strong-coupling asymptotics holds for the Hubbard model in $d = \infty$ as well. It means that there is no difference in leading singular order between impurity and mean-field lattice models at the two-particle critical point.

The exponential asymptotics (26) lies one order false compared with the exact Kondo asymptotics (3). The failure to reproduce the correct Kondo scale disqualifies the simple ring and ladder diagrams as appropriate for intermediate and strong couplings. It is evident from the parallel comparison of two *topologically inequivalent* approximations (rings and ladders) leading to the same low-frequency divergence that in each approximation important diagrams contributing the same divergence were neglected. We hence have to go beyond the simple ladder and ring diagrams in the search for solutions aiming at a reliable description of the transition from weak to strong coupling.

VI. NECESSITY FOR RENORMALIZATION OF THE INTERACTION STRENGTH

Already early studies following the pioneering papers of Suhl and co-workers and Hamann, [24,32] indicated the necessity to go beyond the renormalized RPA and to include vertex renormalizations omitted in the approximation of Suhl. The simple ring and ladder approximations renormalize only the self-energy and use the unrenormalized interaction strength U in scattering processes. It is clear that at intermediate and strong coupling the actual interaction, the quasiparticles effectively feel in their mutual scattering events, must be renormalized by the presence of other quasiparticle pairs. Actually we have to replace the bare interaction U by a renormalized two-particle function $\mathcal{K}_{\uparrow\downarrow}$ from (12) projected to the interaction channel. We will do it systematically in the next section.

However, there is a more basic reason to introduce vertex renormalization whenever we use mass renormalization. There is a relation between a two-particle function and a derivative of the one-particle propagator having the structure of a Ward identity. Baym nad Kadanoff formulated necessary conditions for a many-body theory to fulfill mass conservation. A generalized Ward identity connecting an irreducible vertex function with a variation of the self-energy with respect to an external potential was thereby derived [23]. Interacting electron system contains not only mass but also charge. The electron-electron interaction represents electrostatic energy with $U = e^2/a^*$. In closed systems the electrostatic potential is generated entirely by the actual charge distribution. The charge is carried exclusively by particles involved. Hence a redistribution of mass density must be accompanied by a corresponding charge redistribution in order not to generate spurious sources of the electrostatic potential. This "charge conservation", i.e. the entire electrostatic potential is generated from the charge distribution only, can be expressed for the Hubbard interaction as a "Ward identity"

$$\frac{\partial\Omega(U,\mu_{\mathbf{i}\sigma})}{\partial U} = \sum_{\mathbf{i}}\left[\frac{\delta^2\Omega}{\delta\mu_{\mathbf{i}\uparrow}\delta\mu_{\mathbf{i}\downarrow}} + \frac{\delta\Omega}{\delta\mu_{\mathbf{i}\uparrow}}\frac{\delta\Omega}{\delta\mu_{\mathbf{i}\downarrow}}\right] = \sum_{\mathbf{i}}\left\{\frac{T}{4}[\kappa_{\mathbf{ii}} - \chi_{\mathbf{ii}}] + n_{\mathbf{i}\uparrow}n_{\mathbf{i}\downarrow}\right\} \tag{27a}$$

with grand potential Ω defined in (7) and $\kappa_{\mathbf{ii}}$, $\chi_{\mathbf{ii}}$ as the static, local compressibility and susceptibility, respectively. We can generalize this static identity using small space and time inhomogeneous perturbations $U \to U + \delta U_{\mathbf{ij}}(\tau,\tau')$ and $\mu_\sigma \to \mu_\sigma + \delta\mu_{\mathbf{i}\sigma}(\tau)$ to

$$\left.\frac{\delta\Phi[U,G]}{\delta U_{\mathbf{ij}}(\tau,\tau')}\right|_{\substack{\delta U=0\\ \delta\mu=0}} = -\left.\frac{\delta G_{\mathbf{ii}\uparrow}(\tau,\tau^+)}{\delta\mu_{\mathbf{j}\downarrow}(\tau')}\right|_{\substack{\delta U=0\\ \delta\mu=0}}\,. \tag{27b}$$

Both these identities are fulfilled for an exact solution. The left-hand side of (27b) is the fundamental two-particle function for which the explicit linked-cluster expansion is used. The right-hand side of (27b) makes connection to the dynamical susceptibility and compressibility obtained as a variation of the one-particle Green function. If (27b) is violated we cannot refer to inequality (6). Identity (27b) is important for the linked-cluster expansion where it is used as a fundamental tool for the construction of the generating functional, i.e. for explicit integration in the linked-cluster theorem (9) [33]. However, even for classical spin systems, where the situation is much easier, it was impossible to integrate (27b) in full and to resolve the generating functional Φ completely [34].

Most of the existing self-consistent approximations renormalize only mass, i.e. use renormalized one-electron propagators neglecting vertex renormalization. The Ward identity (27) is always violated in self-consistent theories that do not renormalize interaction strength. E.g. for the Hartree approximation we obtain after a Fourier transform

$$\left.\frac{\delta G_\uparrow^{Hartree}}{\delta \mu_\downarrow}(\mathbf{q}, i\nu_m)\right|_{\substack{\delta U=0\\ \delta\mu=0}} = U X_\uparrow(\mathbf{q}, i\nu_m) X_\downarrow(\mathbf{q}, i\nu_m) \left[1 - U^2 X_\uparrow(\mathbf{q}, i\nu_m) X_\downarrow(\mathbf{q}, i\nu_m)\right]^{-1} \tag{28}$$

with the Hartree one-electron propagators. Since $\Phi^{Hartree} \equiv 0$, identity (27b) is violated by terms proportional to U, the small expansion parameter of the Hartree approximation. Violation of "charge conservation" in the Hartree approximation has no qualitative impact onto the physics of the solution unless there is a phase transition making the right-hand side of (28) diverge. We hence cannot rely upon the Hartree approximation at critical points. The Hartree phase diagram must be confirmed by a more advanced approximation complying better with charge conservation. At least in such a manner that both sides of (27b) lead to qualitatively the same phase diagram.

To improve the Hartree approximation towards charge conservation we use the right-hand side of (28) for the determination of the generating functional $\Phi[U, G]$ from the linked-cluster theorem. We end up with a generating functional of the ring diagrams investigated in Sec. IV A. Since neither this approximation contains vertex renormalizations, we cannot expect Ward identity (27) to be fulfilled [29]. The left-hand side of (27b) for the ring diagrams is identical with the right-hand side of (28) where the Hartree propagators are replaced by those from the ring diagrams. The new right-hand side of identity (27b) must be determined from a set of integral equations and becomes a complicated function of irreducible vertex functions $\delta\Sigma_\sigma/\delta G_{\sigma'}$. The integral equation without integration variables can formally be written as

$$\begin{aligned}&\left\{\left[1 - G_\uparrow G_\uparrow \frac{\delta\Sigma_\uparrow}{\delta G_\uparrow}\right]\left[1 - G_\downarrow G_\downarrow \frac{\delta\Sigma_\downarrow}{\delta G_\downarrow}\right] - G_\uparrow G_\uparrow \left[U + \frac{\delta\Sigma_\uparrow}{\delta G_\downarrow}\right] G_\downarrow G_\downarrow \left[U + \frac{\delta\Sigma_\downarrow}{\delta G_\uparrow}\right]\right\}\frac{\delta G_\uparrow^{Ring}}{\delta\mu_\downarrow} = \\ &-G_\uparrow G_\uparrow \left[U + \frac{\delta\Sigma_\uparrow}{\delta G_\downarrow}\right] G_\downarrow G_\downarrow\end{aligned} \tag{29}$$

The vertex functions $\delta\Sigma_\sigma/\delta G_{\sigma'}$ contain first ladder terms with interaction lines renormalized due to electron-hole polarization bubbles, cf. Fig. 3. We see that to comply with charge conservation at least all ladder and ring diagrams must be taken into account. We can continue iterations beyond the ring diagrams by correcting the two-particle function $\mathcal{C}(\mathbf{q}, i\nu_m)$ using (29). From the new function $\mathcal{C}(\mathbf{q}, i\nu_m)$ we derive the new self-energy and the vertex functions $\delta\Sigma_\sigma/\delta G_{\sigma'}$. They again generate new corrections to $\mathcal{C}(\mathbf{q}, i\nu_m)$ and the iterations can continue till the convergence is reached. Already the initial two steps of this iteration scheme indicate that first the parquet diagrams can be expected to satisfy identity (27).

The parquet algebra is very complicated and does not allow for a general self-consistent (non-perturbative) solution. If all simpler approximations break identity (27) we may ask how much the violation of charge conservation matters. It is physically *inacceptable* if the functions from the right and left-hand sides of equation (27) generate *qualitatively* different phase diagrams and lead to incompatible spectral properties. We can trust an approximation violating (27) only if both sides of (27b) are qualitatively equivalent or if the next step in the iteration scheme towards charge conservation corroborates the results of the chosen approximation. E.g. the phase diagram of the Hartree approximation can be relied upon if it is confirmed by the ring diagrams. Phase transitions calculated with the ring diagrams can be seen as justified if the vertex functions $\delta\Sigma_\sigma/\delta G_{\sigma'}$ do not contain non-integrable singularities that would generate new singularities in integral equation (29).

VII. DIPOLE APPROXIMATION

It follows from preceding analysis that the full parquet approximation would be an ideal candidate for a theory interpolating between weak and strong coupling. It renormalizes the interaction strength to comply with charge conservation, at least qualitatively. It can be expected to possess appropriate asymptotic behavior in both the extreme limits. We, however, also learned that only nonperturbative solutions, treating singularities of two-particle functions at intermediate coupling analytically, can lead to numerically stable solutions for arbitrary interaction strength. Parquet diagrams were studied in connection with the local-moment problem as improvements of Suhl's approximation. Since no exact solutions to the parquet equations exist, approximations had to be used. The local ansatz chosen in [24] failed to reproduce the Kondo scale at strong coupling. Neither non-self-consistent analysis of divergent diagrams at strong-coupling [32] helped in the selection of the relevant classes of diagrams. To achieve a feasible extension of the simple approximations from Sec. IV appropriate for the description of the metal-insulator transition we must reduce the full parquet algebra. Since the scatterings in the electron-hole and interaction channels contribute the same divergence at the critical point we must involve the two channels self-consistently. To do that we propose a new approximation scheme backed by physical reasoning selecting relevant scattering processes leading to the creation of neutral "dipole" bound pairs.

In the critical region of the metal-insulator transition we expect that electrons and holes with opposite spins, i.e. singlets, form pairs of almost bound states. It means that if an electron and a hole with opposite spins get close to each other they tend to stay together for macroscopically long times. Probability of mutual scatterings of electrons and holes with opposite spins is hence much higher than other scattering events. The *intra-pair* scatterings of the electron and hole from the binding pairs are pronounced and are mediated by a renormalized interaction due to the presence of other almost bound electron-hole pairs. The pairs have the total charge zero and carry only a dipole moment. The *inter-pair* interaction is of dipole character and hence weak. There is no significant renormalization of the electrostatic potential in scarce interaction processes between pairs or pairs and particles. The dipole approximation hence systematically neglects all multiple scatterings where more than two particles take part.

This intuitive physical picture can mathematically be formulated in terms of specific approximations in the general parquet algebra (12). First of all the three-particle and higher-order irreducible diagrams are neglected, i.e. the completely irreducible function $I_{\uparrow\downarrow} = U$. Next, the triplet scatterings are neglected in favor of singlet scatterings. We can put in the asymptotic limit of the metal-insulator transition

$$\Lambda^{\alpha}_{\sigma\sigma}(k, k'; q) = 0 \tag{30a}$$

where $\alpha = U, ee, eh$. This approximation enables us to solve the parquet equations (12) in the vertical, interaction channel. The two-particle function from the vertical channel, i.e. $\mathcal{K}^{v}_{\uparrow\downarrow}(k, k'; q) = U + \mathcal{K}^{U}_{\uparrow\downarrow}(k, k'; q)$ becomes a functional of the two-particle scattering function from the horizontal channel defined as

$$\Lambda^{U}_{\uparrow\downarrow}(k, k'; q) = \mathcal{K}^{h}_{\uparrow\downarrow}(k, k'; q) = U + \mathcal{K}^{eh}_{\uparrow\downarrow}(k, k'; q) + \mathcal{K}^{ee}_{\uparrow\downarrow}(k, k'; q)\,. \tag{30b}$$

In the critical region of the metal-insulator transition the two-particle scattering functions $\mathcal{K}^{eh}_{\uparrow\downarrow}(k, k'; q)$ and $\mathcal{K}^{U}_{\uparrow\downarrow}(k, k'; q)$ show divergence for $\mathbf{q} = \mathbf{q_0}$ and $\nu \to 0$. This divergence is smeared out whenever we build convolution of these functions connected only by corresponding electron propagators. Only if we interject bare interaction U between any convolution of reducible functions from both horizontal and vertical channels the divergence survives in leading-order also in convolutions. This restriction reflects the physical fact that multiple scatterings of bound pairs with other pairs or fermions are negligible at the critical point where bound electron-hole pairs condense. Taking this into account we obtain a solution for $\mathcal{K}^{v}_{\uparrow\downarrow}(k, k'; q)$ in closed form and independent of the fermionic four-momenta k, k'

$$\mathcal{K}^{v}_{\uparrow\downarrow}(k, k'; q) = \Gamma_{\uparrow\downarrow}(\mathbf{q}, i\nu_m) = \frac{U}{1 - U\Lambda(\mathbf{q}, i\nu_m)}\,. \tag{30c}$$

The pair function $\Lambda(\mathbf{q}, i\nu_m)$ is a sum of irreducible diagrams that cannot be split into two separate components of the same character by cutting the interaction line. Typical diagrams included and omitted in the renormalized interaction $\Gamma_{\uparrow\downarrow}$ are plotted in Fig. 4. The irreducible function $\Lambda(\mathbf{q}, i\nu_m)$ is connected with the two-particle scattering function $\mathcal{K}^{h}_{\uparrow\downarrow}(k', k''; q)$ analogously to (10)

$$\Lambda(q) = \frac{1}{\beta^2\mathcal{N}^2}\sum_{k',k''} G_\uparrow(k')G_\uparrow(k'+q)G_\downarrow(k'')G_\downarrow(k''+q)\mathcal{K}^h_{\uparrow\downarrow}(k',k'';q)\,. \tag{30d}$$

To complete the approximation we must specify the two-particle function from the horizontal channel. It is determined from equations (12a) and (12b) with appropriate irreducible functions. Since multiple electron-electron scatterings do not contribute divergent terms in the critical region of the metal-insulator transition we can neglect these scatterings completely without affecting leading-order asymptotics. We can write

$$\Lambda^{eh}_{\uparrow\downarrow}(k,k';q) = \Gamma_{\uparrow\downarrow}(q) \quad , \quad \Lambda^{ee}_{\uparrow\downarrow}(k,k';q) = 0\,. \tag{31}$$

The parquet algebra is now complete, i.e. (31) and (12b) fully characterize $\mathcal{K}^{eh}_{\uparrow\downarrow}(k',k'';q)$. To construct the generating functional we rewrite relation (10) between the two-particle scattering function $\mathcal{K}$ and the correlation function $\mathcal{C}$ in our simplified parquet algebra to

$$\mathcal{C}(\mathbf{q},i\nu_m) = \frac{\Lambda(\mathbf{q},i\nu_m)}{1-U\Lambda(\mathbf{q},i\nu_m)}\,. \tag{32}$$

Using these equations and linked-cluster theorem (9) we obtain the functional of the grand potential

$$\begin{aligned}\frac{1}{\mathcal{N}}\Omega[n;\Sigma,G] = -Un_\uparrow n_\downarrow - \frac{1}{\beta\mathcal{N}}\sum_{\sigma n,\mathbf{k}} e^{i\omega_n 0^+}\left\{\ln\left[i\omega_n+\mu_\sigma-\epsilon(\mathbf{k})-Un_{-\sigma}-\Sigma_\sigma(\mathbf{k},i\omega_n)\right]\right.\\ \left.+G_\sigma(\mathbf{k},i\omega_n)\Sigma_\sigma(\mathbf{k},i\omega_n)\right\} + \frac{U}{\beta\mathcal{N}}\sum_{\mathbf{q}m} e^{i\nu_m 0^+}\int_0^1 d\lambda\frac{\Lambda[G](U\lambda|\mathbf{q},i\nu_m)}{1-U\lambda\Lambda[G](U\lambda|\mathbf{q},i\nu_m)}\,.\end{aligned} \tag{33}$$

Eqs. (30)-(33) fully determine the thermodynamic as well as the spectral properties of the dipole approximation for arbitrary interaction. They represent an asymptotic solution of the parquet diagrams in the critical region of the metal-insulator transition, $U \nearrow U_c$, where electron-hole bound pairs condense.

It is still a tremendous task to solve the above equations in the whole range of the coupling constant. In the weak-coupling limit it reduces to a sum of RPA and ring diagrams, i.e. to a FLEX approximation [35]. In the strong-coupling limit the function $\Gamma_{\uparrow\downarrow}(q)$ develops a pole at the Fermi energy and we can use the low-energy expansion as demonstrated for simple approximations in Sec. V. In the critical region of the metal-insulator transition $U \to U_c$ we can replace in leading order the function $\Lambda(U\lambda)$ in the grand potential by $\Lambda(U)$. We can integrate over the interaction strength to obtain the generating functional in closed form

$$\Phi[U,G] \doteq \frac{1}{\beta\mathcal{N}}\sum_{\mathbf{q}m} e^{i\nu_m 0^+}\ln\left[1-U\Lambda[G](U|\mathbf{q},i\nu_m)\right]\,. \tag{34}$$

Note that (34) differs from the generating functional (15a) by a factor of two due to the fact that in the critical region we sum up equivalent contributions from the ring as well as from the ladder diagrams. The weak coupling limit of (34) does not hence reproduce leading-order term in U with the correct weight.

The final step in our approximation in the critical region of the metal-insulator transition is the low-energy ansatz enabling to treat the singularity in $\mathcal{C}(\mathbf{q},\zeta)$ analytically. At the mean-field level, where no momentum integration appears, we use

$$\Lambda(\zeta) \doteq \Lambda_0 + i\,\mathrm{sign}(\mathrm{Im}\zeta)\Lambda'\zeta\,. \tag{35}$$

We introduced two real and positive "mean-field" parameters Λ_0 and Λ' that are to be determined from equations (30)-(33) with the above ansatz in the function $\Gamma_{\uparrow\downarrow}(\zeta)$. Note that there are no closed equations for Λ_0 and Λ' derivable from a generating functional. It means that all physical quantities or equations for them must be determined from the full grand potential (33), (34). The low-frequency ansatz (35) must be applied only at the end stage of the evaluation or solution. It is important that contrary to the simple approximations the dynamical vertex renormalization Λ' is now a nontrivial function of the interaction strength. This is a minimal condition a theory must fulfill if metal-insulator transition should be described [36].

We are now in a position to perform quantitative analysis of the dipole approximation in the critical region of the metal-insulator transition. All the singularities in this approximation are generated by the single function $\Gamma_{\uparrow\downarrow}(\zeta)$. With the low-frequency ansatz (35) we get the singularities under control. It enables us to follow the solution from the weak-coupling regime up to the critical interaction where the metal-insulator takes place and to learn the critical behavior at this transition point in detail. However, a number of technical steps must be done before we gain the explicit strong-coupling asymptotics within the dipole approximation. Quantitative analysis and the results of the dipole approximation for the single-impurity Anderson model and the Hubbard mean-field model will hence be presented in the forthcoming paper.

VIII. CONCLUSIONS

We analyzed in this paper correlated electron systems described by single-impurity Anderson and Hubbard models at intermediate and strong couplings. We concentrated on the half-filled case where the Kodo behavior in the former and metal-insulator transition in the latter model are expected. We showed that in both cases a vanishing scale makes numerical solutions unstable and prevents numerical extrapolation of weak-coupling approximations to the strong-coupling limit. Hence neither Kondo strong-coupling asymptotics nor the metal-insulator transition are directly accessible from the weak-coupling (metallic) side. We demonstrated that the vanishing, Kondo, scale has its origin in a pole of an appropriate two-particle Green function. The relevant two-particle function at intermediate coupling is shown to be a dynamical generalization of the two-particle part of the underlying Hamiltonian (4). The pole in this function signals that singlet bound electron-hole pairs condense and turn the half-filled metallic solution insulator.

The vanishing Kondo scale at strong coupling makes quantitative description of this limit difficult. The only way how to get the instabilities connected with this small scale under control is to treat the Kondo scale separately from other scales determined by the Hamiltonian or the input parameters. To this end we proposed a perturbative scheme enabling direct access to two-particle functions. We used a quantum version of a linked-cluster expansion where bonds stand for interaction lines and vertices for loops of fermionic particles (electrons, holes). With the aid of the linked-cluster theorem we succeeded in constructing a generating functional for the parquet diagrams where all three and higher order irreducible functions are neglected. This approximation is a fully self-consistent sum of contributions from vertical (ring) and horizontal (ladder) channels of the full two-particle scattering matrix.

The approximation containing the unrestricted parquet algebra does not allow for a global nonperturbative solution needed in the strong-coupling limit. We analyzed simplified versions of the parquet approximation summing separately either the ring diagrams or the ladders of electron-hole and electron-electron multiple scatterings. These approximations, known as ring approximation, renormalized RPA and TMA, are used to demonstrate the two-particle instability at intermediate coupling. It was shown that the ring and electron-hole ladders lead to the same divergence in the effective quasiparticle mass in the Fermi-liquid regime. We used a low-frequency ansatz to factorize leading-order singularity of the two-particle scattering function. It enabled us to treat the vanishing Kondo scale analytically and separately from the other scales of the interacting system as demanded from numerical stability. The simple ring and ladder approximations were evaluated with the low-frequency ansatz in the strong-coupling limit and the same physically incorrect result for the rings and electron-hole ladders was obtained. The Kondo scale in both cases leads to the dependence $T_K \propto \exp\{-\pi^2 U^2 \nu^2\}$ either in the single-impurity Anderson model or in the Hubbard model in $d = \infty$.

The failure of the simple ring and ladder approximations to the two-particle scattering function to reproduce the Kondo scale in the single-impurity Anderson model or metal-insulator transition in the Hubbard model lies in the lack of vertex corrections or dynamical renormalization of the interaction strength. We used a very general argument, interpreted as Ward identity for charge conservation, connecting variational derivatives of the generating functional with respect to the spin-dependent chemical potentials and the interaction strength. This identity, fulfilled in the exact solution, demands that whenever we renormalize electron mass (one-electron self-energy) we must adequately renormalize charge (interaction strength). We showed that first the full parquet diagrams self-consistently summing ring and ladder diagrams can be expected to fulfill the Ward identity (27).

Any reliable approximation suitable for the description of the transition from weak to strong coupling in interacting electron systems must contain vertex corrections qualitatively equivalent to those

embodied in the parquet algebra. We analyzed the parquet diagrams in the critical region of the metal-insulator transition from the metallic side and developed a dipole approximation. This approximation systematically neglects nonsingular contributions and keeps only leading-order divergent terms of the full two-particle scattering matrix from the parquet approximation. Together with the low-frequency ansatz a feasible approximation was achieved enabling to study the strong-coupling limit of correlated electron systems at a qualitatively new level. Moreover, the dipole approximation obeys Fermi-liquid asymptotics at weak coupling and it can be viewed as a theory of mean-field character interpolating between the weak and strong-coupling limits. Since no important, divergent, diagrams from the parquet diagrams were omitted in the dipole approximation, we may expect that it will correctly reproduce the Kondo strong-coupling behavior of the single-impurity Anderson model and eventually the metal insulator transition in the Hubbard model. Quantitative analysis of the sample models of interacting electrons with the dipole approximation is left to the forthcoming paper.

ACKNOWLEDGMENTS

The work was supported in part by the grant No. 202/95/0008 of the Grant Agency of the Czech Republic. I thank Alexander von Humboldt Foundation for financial support during my stay at the University of Augsburg where part of this work was performed.

---

[1] T. Kasuya and T. Saso, editors, *Theory of Heavy Fermions and Valence Fluctuations*, SSSSS **62**, Springer-Verlag, Berlin, 1985.
[2] J. Hubbard, Proc. Roy. Soc. London A **281**, 401 (1964) and W. F. Brinkman and T. M. Rice, Phys. Rev. B **2**, 4302 (1970).
[3] A. Georges, G. Kotliar, W. Krauth, and M. Rozenberg, Rev. Mod. Phys. **68**, 13 (1996).
[4] M. Jarrell, Phys. Rev. Lett. **69**, 168 (1992).
[5] M. J. Rozenberg, X. Y. Zhang, and G. Kotliar, Phys. Rev. Lett. **69**, 1236 (1992).
[6] A. Georges and W. Krauth, Phys. Rev. Lett. **69**, 1240 (1992).
[7] M. Ulmke, V. Janiš, and D. Vollhardt, Phys. Rev. B **51**, 10411 (1995).
[8] A. Georges and G. Kotliar, Phys. Rev. B **45**, 6479 (1992).
[9] X. Y. Zhang, M. J. Rozenberg, and G. Kotliar, Phys. Rev. Lett. **70**, 1666 (1993).
[10] A. Georges and W. Krauth, Phys. Rev. B **48**, 7167 (1993).
[11] M. J. Rozenberg, G. Kotliar, and X. Y. Zhang, Phys. Rev. B **49**, 10181 (1994).
[12] G. Moeller, Q. Si, G. Kotliar, M. J. Rozenberg, and D. S. Fisher, Phys. Rev. Lett. **74**, 2082 (1995).
[13] W. Metzner and D. Vollhardt, Phys. Rev. Lett. **62**, 324 (1989).
[14] V. Janiš, Z. Phys. B **83**, 227 (1991).
[15] P. Nozières, J. Low Temp. Phys. **17**, 31 (1974).
[16] A. M. Tsvelick and P. B. Wiegman, Adv. Phys. **32**, 453 (1983)
[17] K. G. Wilson, Rev. Mod. Phys. **47**, 773 (1975).
[18] There are theories based on the non-crossing approximation (NCA) that are often used to describe the strong-coupling limit, N. E. Bickers, Rev. Mod. Phys. **59**, 845 (1987). These theories, however, do not reproduce the Fermi-liquid regime at zero temperature and are hence unsuitable for interpolation between weak and strong-coupling limits.
[19] V. Janiš, J. Phys. Cond. Matter **8**, L173 (1996).
[20] V. Janiš and J. Schlipf, Phys. Rev. B **52**, 17119 (1995).
[21] K. Yosida and A. Okiji, Prog. Theor. Phys. **34**, 505 (1965).
[22] G. Baym and L. P. Kadanoff, Phys. Rev. **124**, 287 (1961).
[23] G. Baym, Phys. Rev. **127**, 1391 (1962).
[24] R. A. Weiner, Phys. Rev. Lett. **24**, 1071 (1970) and Phys. Rev. B **4**, 3165 (1971).
[25] A. D. Jackson, A. Lande, and R. A. Smith, Physics Reports **86**, 55 (1982).
[26] B. Menge and E. Müller-Hartmann, Z. Phys. B **82**, 237 (1991).
[27] H. Suhl, Phys. Rev. Lett. **19**, 442 (1967).
[28] J. Kanamori, Progr. Theor. Phys. **30**, 275 (1963).

[29] M. Levine and H. Suhl, Phys. Rev. **171**, 567 (1968). Note that here the violation of charge conservation (27) is referred to as non-conservation of spin.
[30] D. R. Hamann, Phys. Rev. **186**, 549 (1969).
[31] It was argued that the low-frequency expansion (21) may break down in the critical region of the metal insulator transition and non-Fermi-liquid contributions have to be taken into account [19]. The non-Fermi-liquid contributions, i.e. from behind the first extrema in the real part of the self-energy, are again dominated by linear terms leading to the same logarithmic divergences. The only change due to non-Fermi-liquid terms is a renormalization of the parameter X'.
[32] M. T. Béal-Monod and D. L. Mills, Phys. Rev. Lett. **24**, 225 (1970).
[33] M. Wortis, in *Phase Transitions and Critical Phenomena*, edited by C. Domb and M. S. Green, volume 3, p. 121, eq. 8, Academic Press, London, 1974.
[34] M. Wortis, D. Jasnow, and M. A. Moore. Phys. Rev. **185**, 805 (1969).
[35] N. E. Bickers, D. J. Scalapino, and S. R. White. Phys. Rev. Lett. **62**, 961 (1989) and N. E. Bickers and D. J. Scalapino, Ann. Phys. **193**, 206 (1989).
[36] V. Janiš and R. Teplý, Czech. J. Phys. **46**, 633 (1996)

Figure Captions

Fig. 1 Real part of the self-energy of the impurity Anderson model at half filling and zero temperature calculated for the Lorentzian DOS within the ring diagrams from Sec. IV A. The first (sharp) extrema are clearly seen to approach the Fermi energy, ($\omega = 0$), with increasing interaction.

Fig. 2 First few diagrams contributing to the electron-hole, (a), electron-electron, (b), and interaction, (c), channels of the two-particle scattering function.

Fig. 3 New vertex functions generated from functional derivatives of the self-energy from the ring diagrams. The double wavy line is the interaction between spin up and spin down particles, and the double dashed line the same between the particles with the same spin renormalized by ring diagrams. These vertex functions are not contained in the left-hand side of identity (27b) of the ring diagrams.

Fig. 4 Typical diagrams contributing to $\Gamma_{\uparrow\downarrow}$, (a), (b), where no more than two particles take part in multiple scatterings from the irreducible function Λ. Diagram (c) does not contribute to $\Gamma_{\uparrow\downarrow}$, since more than two fermion loops are multiply connected with the interaction line.

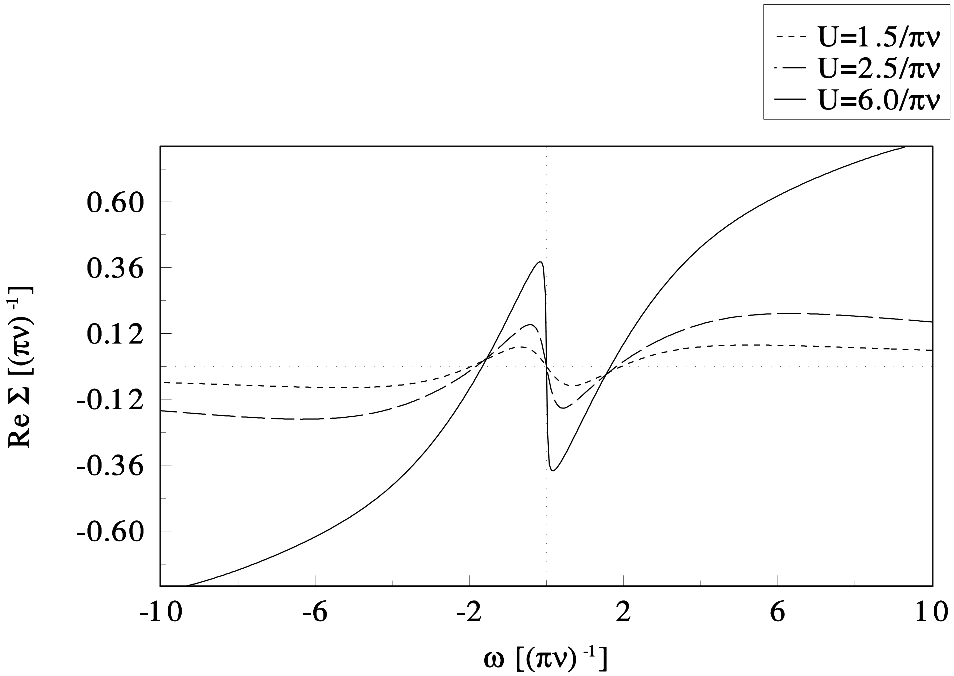

U=1.5/πν
U=2.5/πν
U=6.0/πν
0.60
0.36
0.12
-0.12
-0.36
-0.60
Re Σ [(πν)^-1]
-10
-6
-2
2
6
10
ω [(πν)^-1]

Fig. 1

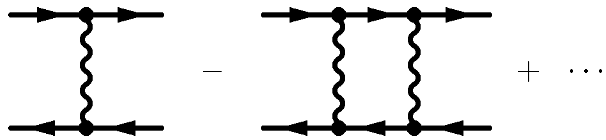

a

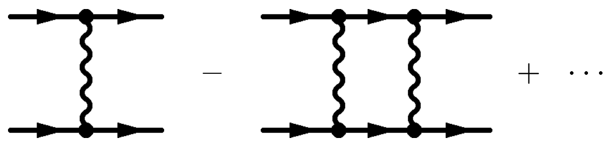

b

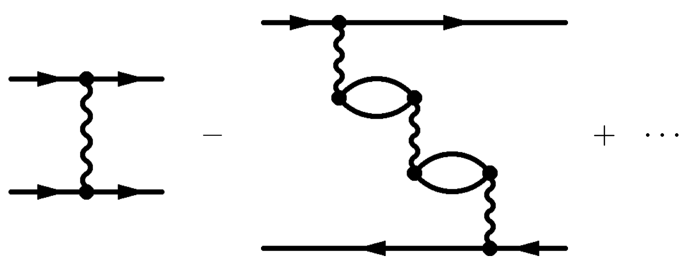

c

Fig. 2

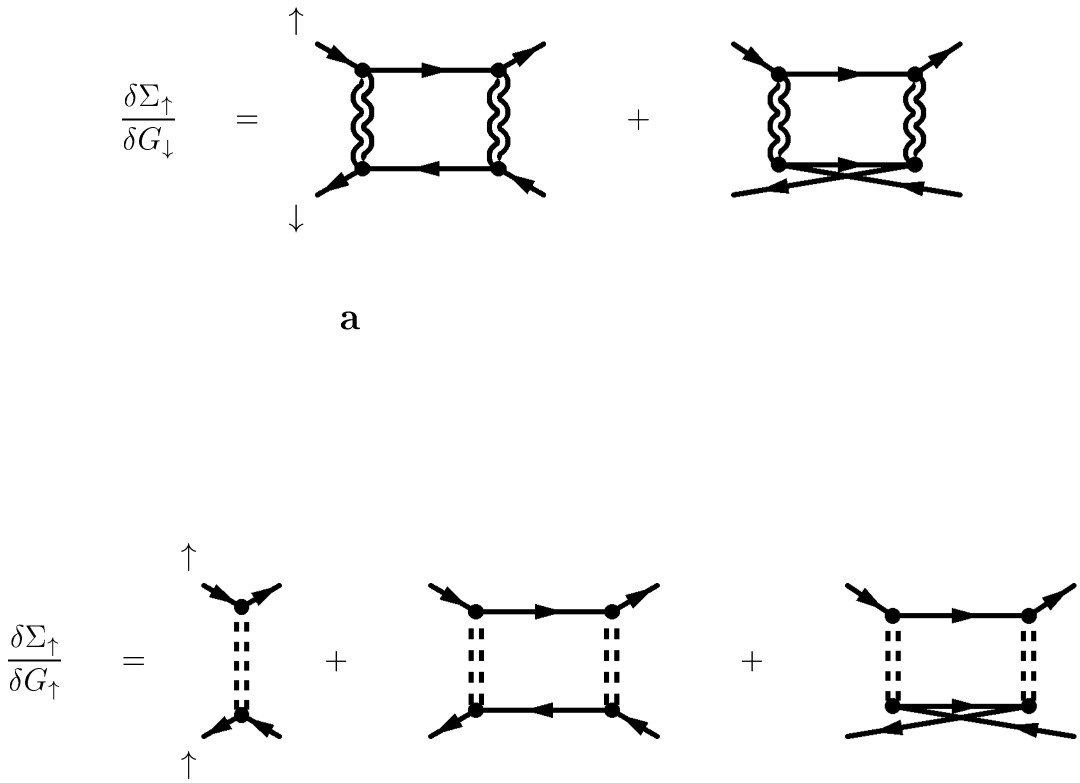

$\frac{\delta\Sigma_\uparrow}{\delta G_\downarrow}$ =
$\frac{\delta\Sigma_\uparrow}{\delta G_\uparrow}$ =

a

b

Fig. 3

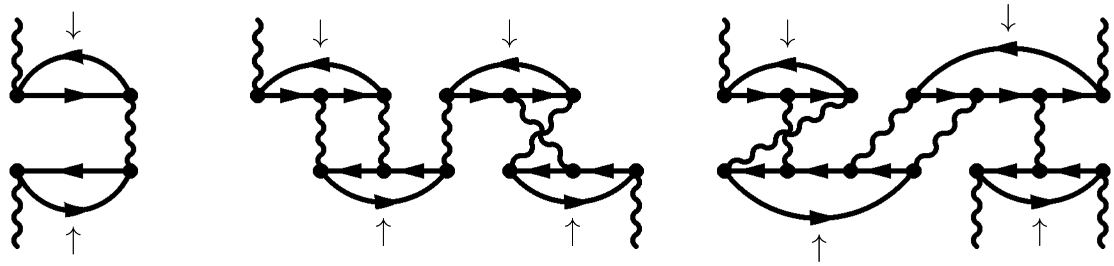

a **b** **c**

Fig. 4